Comparison of AAA and Acuros XB Dose Calculation Algorithms for SRS

by

Feng-Ju Yeh

Graduate Program in Medical Physics
Duke University

Date:_____
Approved:

_____
Zhiheng Wang, Advisor

_____
John Kirkpatrick

_____
Justus Adamson

Thesis submitted in partial fulfillment of the requirements for
the degree of Master of Science in the Graduate Program
in Medical Physics in the Graduate School
of Duke University

2020

المنارة للاستشارات

www.manaraa.com

<u>ABSTRACT</u>

Comparison of AAA and Acuros XB Dose Calculation Algorithms for SRS

by

Feng-Ju Yeh

Graduate Program In Medical Physics
Duke University

Date:_____
Approved:

_____

Zhiheng Wang, Advisor

_____

John Kirkpatrick

_____

Justus Adamson

An abstract of a thesis submitted in partial fulfillment of the requirements for
the degree of Master of Science in the Graduate Program
in Medical Physics in the Graduate School
of Duke University

2020

www.manaraa.com

Abstract

Single isocenter multiple target (SIMT) stereotactic radiosurgery (SRS) provides an effective treatment of brain metastases. However, the delivered dose to the target and the surrounding tissue affect SRS outcomes. The accuracy of dose calculation is a critical challenge in the SIMT SRS application. Two dose calculation algorithms, analytical anisotropic algorithm (AAA) and Acuros XB, have been implemented in a commercial treatment planning system (TPS). The purpose of this project is to compare SIMT SRS dose distribution obtained by Acuros XB dose calculation algorithm and commonly used AAA and to investigate the effects of size, distance to isocenter, and heterogeneity.

Forty clinical cases with 189 targets were used to evaluate the dose distribution differences. All plans were generated using the Eclipse treatment planning system (TPS) V13.6 and calculated using Analytical Anisotropic Algorithm (AAA). Each patient plan consisted of two to 14 targets and treated using volumetric modulated arc therapy (VMAT). These plans were recalculated for the purpose of this project using Acuros XB using the same geometry, voxel resolution, and monitor units. Parameters used for plan comparison included planning tumor volume (PTV) coverage to 99%, 95%, and 1%, PTV minimum dose, PTV mean dose, PTV maximum dose, and whole brain V_{3Gy}, V_{6Gy}, and V_{12Gy}. The dosimetric accuracy was evaluated based on the gamma pass rate with threshold criteria 3%/1mm on SRS MapCHECK.

iv

The two algorithm comparison results showed large dose discrepancies in the PTV minimum dose (-7.9% to 5.3%), also occurring in small field size range and in the small range of distance from PTV to skull. The average difference for $D_{1\%}$, $D_{95\%}$ and $D_{99\%}$ were 0.8%, 0,2% and 0.03%, respectively. However, the difference of $D_{99\%}$ revealed up to -5.7%. Relative to Acuros XB, V_{3Gy}, V_{6Gy} and V_{12Gy} decrease by 1.3%, 0.2% and 2.3% with AAA. Gamma analysis demonstrated a higher gamma pass rate for AAA compared to Acuros XB (99.9%,97.9%).

Dose differences were found in AAA and Acuros XB, particularly in the PTV minimum dose and PTV coverage. Heterogeneity and tumor size introduced uncertainty for dose calculation. However, the dose differences showed no dependence on the distance from isocenter to lesions. AAA showed better agreements between calculated and delivered planar dose distributions than Acuros XB.

Contents

List of Tables

List of Figures

x

1. Introduction

Brain metastases can occur in 20 to 40% of patients with cancer. The number may increase because improving imaging modality provides better tumor detection (Patchell 2003). Stereotactic radiosurgery (SRS) is a technique that utilizes high dose rate and tumor conformity to treat brain metastases. It provides high intracranial disease control and spares superior normal tissue with less cognitive deterioration (Brown 2016, Taso 2012). SRS is recommended to be used as the treatment of 1 to 4 brain metastases (Yamamoto 2014). However, there are limited data regarding the effectiveness of using SRS for patients with larger numbers of brain metastases due to the prohibitively long treatment times when each lesion requires additional shots or separate isocenter(Yamamoto 2014, Jairam 2013). Single-isocenter, multitarget (SIMT), volumetric modulated arc therapy (VMAT) for SRS planning and delivery allows several lesions to be treated simultaneously. It was reported that this technique substantially reduces treatment time while offering possible improvements in target conformity and dose to normal tissue, compared with multiple isocenter plans. (Clark 2010, Kim 2012)

The goal of SRS, including SIMT SRS, is to deliver a highly conformal dose distribution to targets while minimizing the dose to the critical structures such as the brain, brain stem, chiasm, optical nerve, and lenses. These techniques require dose calculation algorithms in terms of accuracy. The accurate dose calculation in the

treatment planning system (TPS) ensures higher target coverage and lower normal tissue toxicity.

Currently, there are various dose calculation algorithms commercially available in clinical routine. The discrepancies in calculated dose exist, especially in the presence of heterogeneity and small field, due to different beam modeling methods. This provides challenges for TPS for dose prediction for brain metastases cases as a result of heterogeneity introduced by bones in the skull and small fields used in the SRS application. The two algorithms, AAA and Acuros XB, have been implemented in the Eclipse treatment planning system for the calculation of dose distribution for photon beams. Routinely, Duke uses AAA for dose calculation.

The AAA was originally developed to meet the clinical expectations, short computation time and high dose calculation accuracy in heterogeneous media for all types of external beam treatments. The AAA is a kernel-based convolution model algorithm. The kernels, describing the dose distribution of secondary particles at the point of interaction and the energy transport, are derived by Monte Carlo particle transport codes. AAA utilizes separate convolution models for primary beams and scattered photons and scattered electrons. The convolutions are applied to many small beamlets into which the beam is divided. The superposition of the dose calculated by photon and electron convolutions for each beamlet allows us to obtain the final dose distribution. The AAA corrects for tissue heterogeneity anisotropically surrounding

2

point irradiation. It employs density scaling of scattering photon kernel for a homogeneous medium, such as water, along with all the lateral directions.

Although AAA improves accuracy in dose calculation significantly, it is still not as good as a Monte-Carlo calculation method which is often believed to predict dose precisely. However, Monte-Carlo calculation takes too much time to be used in routine clinical practice. A new method was introduced as a rapid and accurate alternative to the Monte-Carlo calculation method. This method is Acuros XB, a deterministic algorithm. The Acuros XB applies a deterministic solution of the linear Boltzmann transport equation (LBTE). The advantage of solving LBTE by numerical methods is the absence of statistical noise compared to Monte-Carlo calculation, which indirectly obtains the solution of LBTE through a vast amount of random samplings of particles in the media. Since both approaches obtain dose distribution by solving the LBTE, the calculated dose of Acuros XB is expected to be more similar to Monte-Carlo calculation, widely regarded as the golden standard. Moreover, it takes the effect of heterogeneity into account directly in patient dose calculations

Acuros XB has two reporting modes, that is, dose-to-water, D_w, and dose-to-medium, D_m. The electron fluence depending on energy is used to calculated doses and is based on the properties of the medium. The calculation for D_w and D_m is the same, while the post-processing step for them is different. The step includes that the local electron fluence is multiplied by flux-to-dose response functions in that voxel. A

3

www.manaraa.com

response function based on the medium of the voxel is used for D_m, while a water-based response function is used for D_w. Therefore, having the material map of the patient is essential to calculate doses.

Our purpose in this study is to compare dose calculations of the Acuros XB dose calculation algorithm and widely used AAA for SIMT SRS plans, to investigate the effects of size, distance to isocenter, and heterogeneity as well as to access dosimetric accuracy.

4

2. Materials and Methods

2.1 Patient

This project included 40 patients with 2 to 14 brain metastases who received SIMT SRS for brain tumors between 2016 and 2019 at Duke University Medical Center. The average number of lesions is 4.7 per patient. The PTV volume varies from 0.03 ml to 29.3 ml and the average is 1.5 ml. Patient and tumor characteristics are summarized in table 1.

Among all the patients, 8 patients received 18 Gy in a single fraction (18 Gy/1 F), 23 patients received 20 Gy in a single fraction (20 Gy/1 F), 6 patients received 25 Gy in 5 fractions (25 Gy/5 F), and 3 patients received 27.5 Gy in 5 fractions (27.5 Gy/5 F).

Table 1 Summary of Patient and Tumor Characteristic.

	Mean	Std	Range
Number of Lesions	4.7	2.7	(2 , 14)
PTV Volume (ml)	1.5	3.8	(0.03 , 29.3)
Distance to Isocenter (cm)	4.4	1.8	(0.7 , 8.7)
Distance to Skull (cm)	0.9	1.1	(0 , 5.5)

5

2.2 Treatment planning system and dose calculation algorithms

Treatment planning system used in this project was Eclipse (Varian Medical Systems, Palo Alto, CA). The dose calculation algorithms were Acuros XB (V15.6) and AAA (V13.6) with heterogeneity correction. The calculation grid size was 1 mm. Acuros XB used dose-to-medium and dose-to-water dose reporting modes to calculate doses.

2.3 Comparison of plans

Clinical plans with AAA calculation algorithm were used for comparison. Plans with Acuros XB algorithm were retrospectively generated from clinical plan s with AAA algorithm and the dose distributions were recalculated by Acuros XB.

2.3.1 Original Clinical plans

Patients underwent MRI scan and CT simulation with U-frame mask or frameless mask. A cranial localizer box with cross-sectional rods inside was mounted to the mask. Through identifying the position of cross-sectional rods, CT images with a slice thickness of 1 mm or 1.25mm were fused with contrast-enhanced T1-weighted MRI images. Gross tumor volume (GTV) was delineated based on the fused CT and MRI images. Margins of 1 mm in all direction were added to create a PTV.

Patients were contoured using the BrainLAB iPlan RT Image software (BrainLAB, AG, Munich, Germany). The physician contoured lesions and the physicist contoured critical structures. The dose was normalized such that at least 99% PTV is covered by 100% isodose line. The maximum dose range fall between 110% and 120%. In

6

other words, doses were prescribed to the 80-90% isodose line normalized to the

maximum dose. The prescription doses were determined based on lesion size and

location. Typically, 1 fraction of 18 or 20 Gy is delivered to small lesions while 5 fractions

of 5 or 5.5 Gy is delivered to large lesions. Critical structure dose limits are determined

from QUANTEC on the central nervous system. The plans were optimized using AAA

dose calculation algorithms.

Patients were treated on a Varian Novalis Tx and a Varian TrueBeam STX with

high-definition 120-leaf MLCs (HD120 MLC). HD120 MLC consists of 120 leaves (60

pairs). 32 pairs of 2.5 mm in the center and 28 pairs of 5 mm on each side. 6 MV beams

and VMAT technique (Varian, 2013) were used. Image guidance systems used

orthogonal kV imaging and cone beam CT to make 6-degree-of-freedom position shifts

prior to treatment.

2.3.2 Acuros XB plans

Acuros XB plans were re-calculated as dose to medium with Acuros XB version

15.6, using the same MU and geometry as for the AAA plans. The structure set was the

same as the one used in AAA plans. A physical material table, used in dose calculation,

has to be assigned to the structure set. Finally, the dose was re-calculated. This was

repeated for all AAA plans.

7

2.4 Plan Analysis

To compare dose distribution, quantitative metrics were selected as follows. For plan evaluation, conformity index (CI), heterogeneity index (HI) and dose coverage to PTV were computed. PTV minimum dose, PTV mean dose, PTV maximum dose were recorded to observe dose variation. The volume of brain receiving 3, 6, and 12 Gy was recorded to evaluate low dose regions.

The significance of the difference for each metric between AAA and Acuros XB plans was analyzed by the paired t-test. P value less than 0.05 is defined as statistical significance.

2.4.1 Conformity index (CI)

The Radiation Therapy Oncology Group (RTOG) proposed that conformity index (CI) is a widely used metric which can be employed to describe the quality of SRS plans (1993 Shaw). It is given by:

$$CI = \frac{V_{RI}}{TV}$$

Where V_{RI} is the tissue volume which receive the prescription dose (2007 Eichler) and TV is the target volume, PTV. To obtain the target volume, we opened patient's plan in Eclipse, right clicked the "PTV_all" or "PTV_combined" structure and chose " Measure Volume" to measure the volume. If "PTV_all" or "PTV_combined" structure was not contoured, the volumes of all targets were measured and summed up. To obtain the prescription isodose volume, we right clicked "Dose" and selected "Convert Isodose

8

Level to Structure…" Then, a prescription isodose structure can be created by inputting the parameter "100%" and measured. This was repeated for all plans.

CI values between 1.0 and 2.0 indicates that plans are not deviating from RTOG protocol. CI values between 2.0 and 2.5 or between 0.9 and 1.0 indicate that plans have minor deviations. CI values greater than 2.5 or less than 0.9 indicate that plans have major deviations (1993 Shaw).

2.4.2 Homogeneity index (HI)

RTOG proposed that homogeneity index (HI) is a metric to analyze dose distribution's uniformity in the target volume (1993 Shaw). It is defined by the equation:

$$HI = \frac{I_{max}}{RI}$$

Where I_{max} is the maximum point dose in the target and RI is the reference isodose (2006 Feuvert). In Eclipse, the plan-related information showed on the bottom of the screen. The "Dose Statistic" tab provided the maximum dose of all structures. We used prescription dose to the target as the reference isodose.

HI values less than or equal to 2 imply that the plans are not deviate from protocol. HI values between 2 and 2.5 imply that plans have minor deviations. Major deviations result are found when the value is greater than 2.5 (1993 Shaw).

2.4.3 Volumetric Parameters

V_{3Gy}, V_{5Gy}, and V_{12Gy} are the total volume of the brain receiving 3 Gy, 6 Gy, and 12 Gy, respectively, excluding PTV volume. They are used to evaluate the low dose spread

9

and the toxicities to normal tissues. Lesion coverage, the percent volume of PTV that is encompassed by the 100% isodose line, was also recorded for each metastasis from dose-volume histograms by the method described above.

2.4.4 Dosimetric Parameters

Minimum, mean and maximum doses to the targets were recorded. For PTV coverage, relevant parameters were determined from dose-volume histograms. $D_{99\%}$ (the dose to 99% of the PTV), $D_{98\%}$ (the dose to 98% of the PTV), and $D_{1\%}$ (dose to 1% of the PTV) were evaluated.

2.5 Effects of tumor characteristics

In order to evaluate the effects of tumor size, distance from isocenter to target and distance from target to bone, the scatter plots for each characteristic were created.

2.6 Dosimetry accuracy evaluation

The dosimetry accuracy was evaluated based on the gamma passing rate and dose difference. The measurement was performed by SRSMapCHECK and StereoPHAN.

2.6.1 Equipment

SRSMapCHECK (Sun Nuclear, Melbourne, FL, USA) is a 2D diode array detector consisting of 1013 diodes in a 77 mm by 77 mm array.(Figure 1)The detector spacing is 2.47 mm. The active area of each diode is 0.5 mm by 0.5 mm. These characteristic provide high resolution and allow us to obtain 2D dose distribution and point dose. The

10

diodes are located 2.2 cm below the surface of SRSMapCHECK. The inherent buildup to the detectors is 2.75 g/cm^2.

Figure 1 SRS MapCHECK

StereoPHAN (Sun Nuclear, Melbourne, FL, USA) is made of Polymethyl methacrylate (PMMA). Images of the phantoms are depicted in Figure 2. The sphere shape of phantom provides scatter geometry and angular corrections.
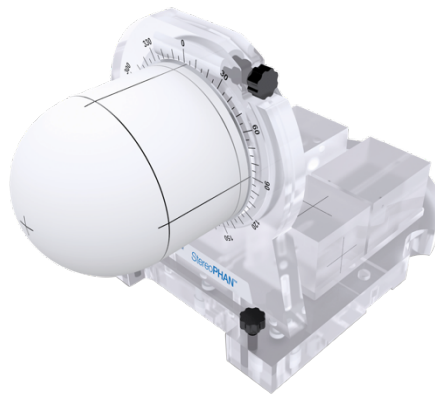
Figure 2 StereoPHAN

Sun Nuclear Corporation (SNC) Patient Software (Sun Nuclear, Melbourne, FL, USA) is a software used in Quality Assurance (QA) and installed on a personal computer. It is used in conjunction with SRSMapCHECK, which is connected to the

11

personal computer via USB. SNC Patient Software can compare measured doses and planned doses. The relative to absolute dose data are compared as well by using Gamma Analysis.

2.6.2 Measurement

In Eclipse, verification plans for each clinical plan were created. The structure set used in verification plans was contoured based on the CT images of StereoPHAN. To prevent SRSMapCHECK's critical electronics from being irradiated, non-coplannar couch kick should not exceed 45 degree. The isocenter is default to (0,0,0). When measuring the dose distribution of an off-center lesion, we moved the isocenter at the time of dose calculation. After doses were calculated, the approved the plan and plan dose were export as DICOM files.

DICOM files were loaded on SNC Patient Software. StereoPHAN angle was set to 0 degree which was the same as the phantom set-up and the user origin of StereoPHAN was matched with SNC software coordinate system. Next, the planned 2D dose distribution was shown on the right side of the screen (Figure 4).

The SRSMapCHECK was inserted into StereoPHAN and two build-up slabs were placed above and under the detector. The phantom was set up to isocenter by indexing bar. (Figure 3) When measuring off-center lesions, a couch shift was added. The device was connected to the personal computer and the successful connection triggered the background measurement.

12
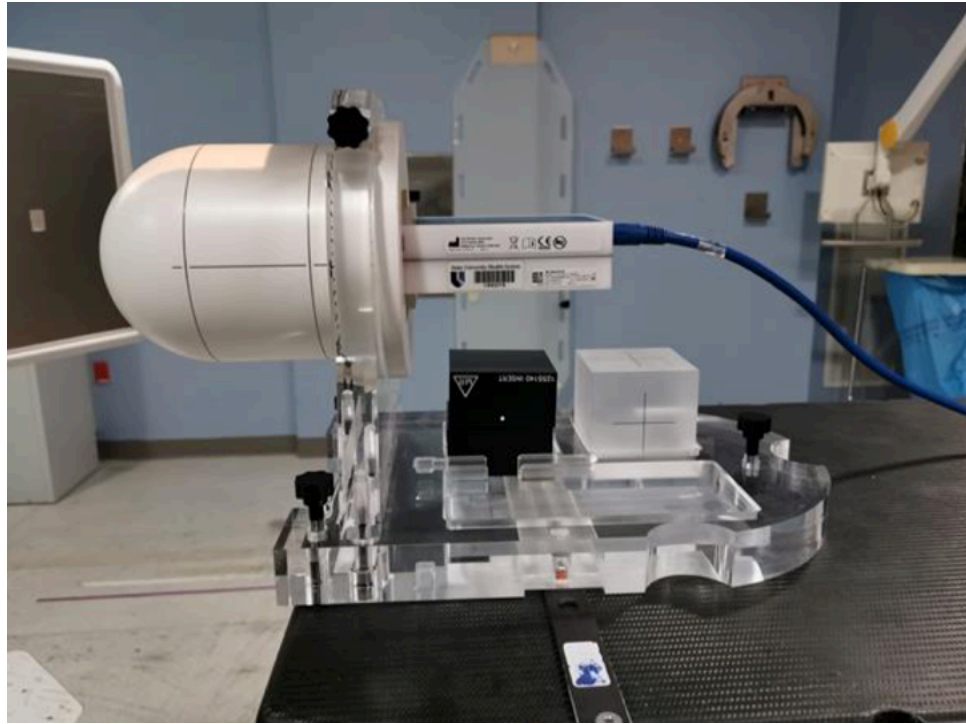
Figure 3 The setup of SRS MapCHECK and StereoPHAN

The dose was measured when the plan was delivered. The measured 2D dose distribution was shown on the left side of the screen (Figure 4). The gamma analysis and dose difference analysis were performed within the software. Each point dose was recorded as well.

المنارة للاستشارات

www.manaraa.com
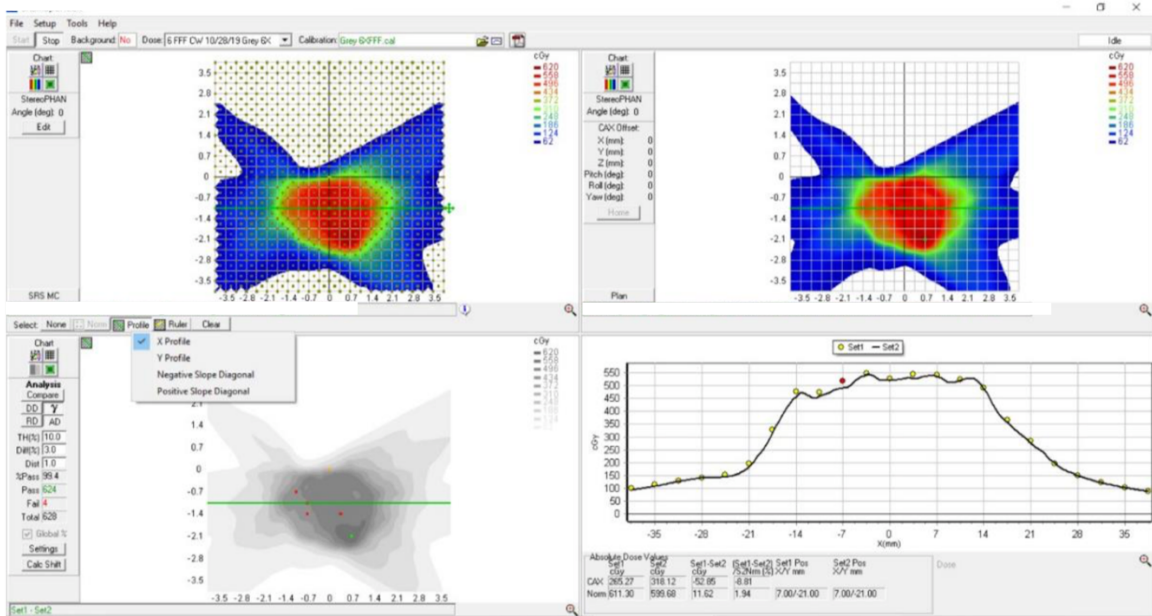
Figure 4 Workspace on SNC Patient Software. Top left of the screen shows the measured 2D dose distribution of a lesion. Top right of the screen shows the planned 2D dose distribution. Bottom right of the screen shows the dose profile along the green line on the bottom left of the screen.

2.6.3 Dose Difference for lesions of interested

After the dose distribution of a lesion was obtained, the maximum point dose was determined. The mean dose was then computed for all point measurements above a threshold of 80% of the maximum dose, and compared to the same value for the dose distribution calculated by the dose calculation algorithms. This was repeated for all lesions of interest.

2.6.4 Gamma Analysis

Gamma index is used for comparison between two dose distributions. It takes into account both dose difference and misalignment. These two factors are collapse into one parameter, gamma (1998 Low). The gamma can be expressed as:

14

$$\Gamma = \sqrt{\left(\frac{DTA}{C_{DTA}}\right)^2 + \left(\frac{DD}{C_{DD}}\right)^2}$$

Where C_{DTA} and C_{DD} are the acceptance criteria of distance-to-agreement (DTA) and dose difference (DD). They are set to 3% and 1 mm. When the minimum of Γ is less than or equal to 1, the dose calculation of a point passes; while it is more than 1, the dose calculation fails. The gamma pass rate was computed based on the pass-fail results of each point.

15

3. Results

3.1 Clinical plans

3.1.1 Comparison for targets

A summary of the dosimetric metric differences for PTVs is given in Table 2. The differences occurred in dose distribution between the AAA and Acuros XB. For d_m and AAA, the maximum difference of PTV minimum dose was -7.91%. The maximum difference of $D_{99\%}$ was -6.13%. The results in Table 3 also show the statistical significance difference between algorithms for CI (p=0.007), HI (p<0.0001) and, coverage (p=0.0140). The maximum differences for CI and coverage are -26.87% and -28.%, respectively.

For d_w and AAA, the maximum difference of PTV maximum dose was 10.75%. The maximum difference of $D_{1\%}$ was 9.31%. The results in Table 3 also show the statistical significance difference between algorithms for CI(p<0.0001), HI (p<0.0001) and, coverage (p<0.0001). All the mean differences between AAA and Acuros XB d_w are larger than the differences between AAA and Acuros XB d_m.

Figure 5 displays the comparison of DVH between AAA and Acuros XB d_w. Figure 6 displays the comparison of DVH between AAA and Acuros XB d_m. From these figures, AAA's prediction is more similar to the prediction of Acuros XB d_m than the one of Acuros XB d_w.

Figure 7 displays the distribution of the PTV dose difference between AAA and Acuros XB(d_m) for all patients. The distributions of PTV minimum dose difference and

16

PTV mean dose difference are symmetric, while the distribution of PTV maximum dose difference is positively skewed. The PTV minimum dose difference is more dispersed than the others. All the differences of outliers were negative, that is, AAA plans had higher dose prediction. Figure 8 displays distributions of $D_{1\%}$, $D_{95\%}$ and, $D_{99\%}$. $D_{99\%}$ is negatively skewed and more dispersed. $D_{95\%}$ have the most outliers. Their differences are all negative.

Figure 9 displays the distribution of the PTV dose difference between AAA and Acuros XB(d_w) for all patients. All the distributions are symmetric. The PTV mean dose difference is less dispersed than the others. Most the differences of outliers were positive, that is, Acuros XB(d_w) plans had higher dose prediction. Figure 10 displays distributions of $D_{1\%}$, $D_{95\%}$ and, $D_{99\%}$. $D_{1\%}$ is positively skewed and has more dispersed. $D_{1\%}$ also have the most outliers. Their differences are all positive.

Figure 11 to Figure 12 display the correlation between PTV dose difference (Acuros XB_d_m-AAA) and distance from isocenter to target. No correlation is observed. Figure 15 to Figure 16 display the correlation between PTV dose difference (Acuros XB_d_m-AAA) and size. The differences between small tumors (smaller than 5 ml) vary from 0% up to -8% and 5%. Figure 19 to Figure 20 display the correlation between PTV dose difference (Acuros XB_d_m-AAA) and the minimum distance from target to bones. Hence, small tumors and near bone location introduce uncertainties in dose calculation.

17

Figure 13 to Figure 14 display the correlation between PTV dose difference (Acuros XB_d_w-AAA) and distance from isocenter to target. Figure 17 to Figure 18 display the correlation between PTV dose difference (Acuros XB_d_w-AAA) and size. Figure 21 to Figure 22 display the correlation between PTV dose difference (Acuros XB_d_w-AAA) and the minimum distance from target to bones. No correlation is observed

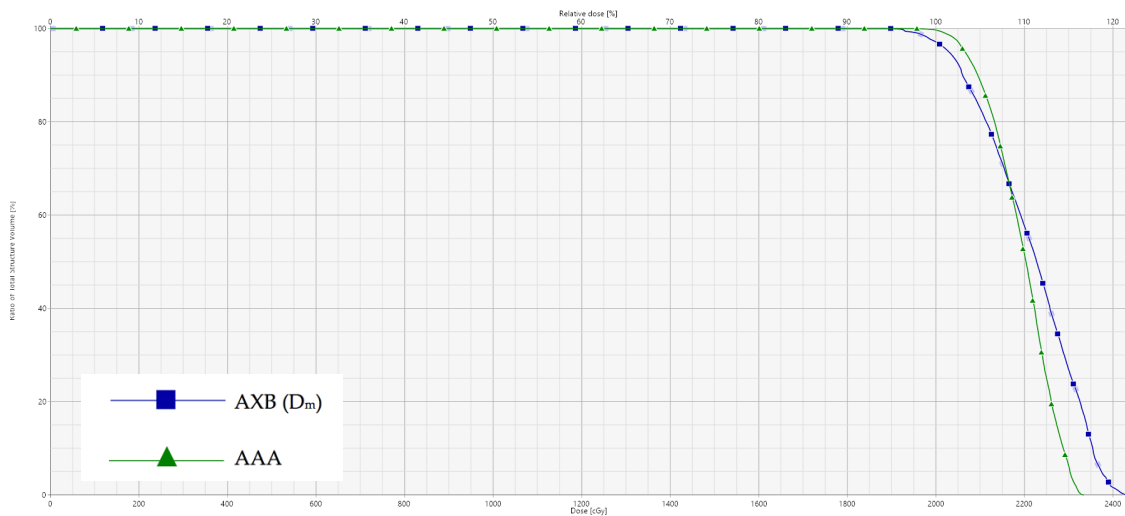**Table 2 Comparison between AAA and Acuros XB for PTVs**

	Relative difference (AXB_D_m-AAA)/AAA*100% Mean ± Std (min-max)	P value	Relative difference (AXB_D_w-AAA)/AAA*100% Mean ± Std (min-max)	P value
PTV				
$D_{1\%}$	0.80 ± 1.54 (-3.91 , 4.43)	<0.0001	2.72 ± 2.03 (-7.49 , 9.31)	<0.0001
$D_{95\%}$	0.24 ±1.75 (-5.69 , 3.24)	0.00756	2.28 ± 1.16 (-0.26 , 5.68)	<0.0001
$D_{99\%}$	-0.03 ± 1.95 (-6.13 , 3.79)	0.34578	2.11 ± 1.22 (-1.36 , 5.21)	<0.0001
Min	-0.23 ± 2.41 (-7.91 , 5.29)	0.7705	1.91 ± 1.99 (-2.98 , 7.17)	<0.0001
Max	0.62 ± 1.74 (-4.52 , 4.54)	0.0003	2.74 ± 2.17 (-2.57 , 10.75)	<0.0001
Mean	0.74 ± 1.38 (-3.45 , 3.41)	<0.0001	2.58 ± 1.33 (-1.29 , 7.63)	<0.0001

**Table 3 Comparison between AAA and Acuros XB for plan quality**

	Relative difference (AXB_D_m-AAA)/AAA*100% Mean ± Std (min-max)	P value	Relative difference (AXB_D_w-AAA)/AAA*100% Mean ± Std (min-max)	P value
CI	-0.72 ± 9.96(-26.87 , 16.71)	0.007	16.61 ± 8.77(3.63 , 41.06)	<0.0001
HI	0.62 ± 1.73 (-4.52 , 4.54)	<0.0001	2.74 ± 2.17 (-2.56 , 10.75)	<0.0001
Coverage	-0.67 ± 3.29 (-28.36 , 13.40)	0.0140	0.43 ± 1.10 (-0.30 , 11.37)	<0.0001
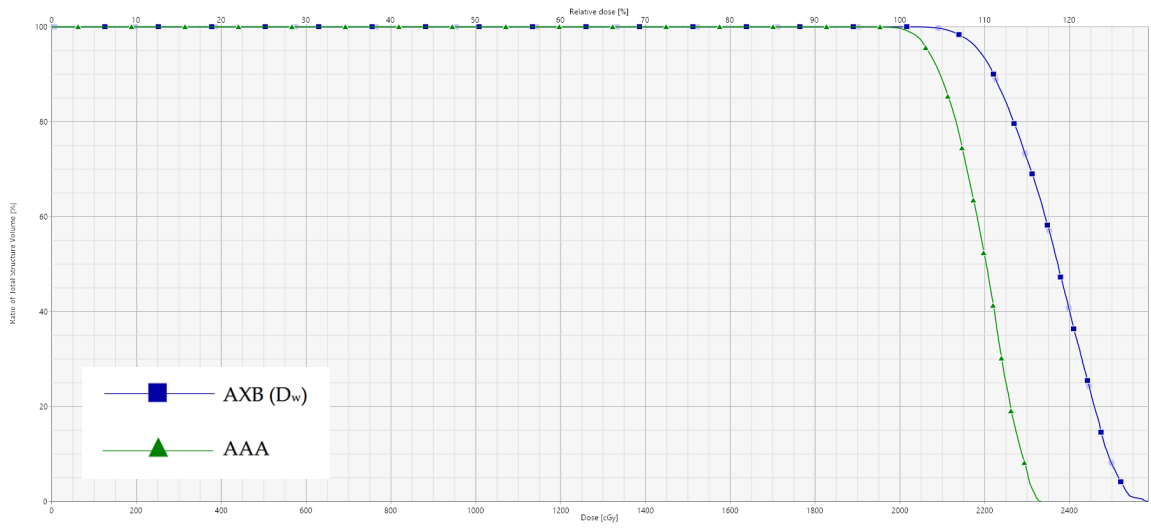
**Figure 5 An example DVH comparison of PTV doses between AAA and Acuros XB(Dw). The dose difference of PTV minimum dose, maximum dose, and mean dose was 5.24%, 10.2% and 7.35%, respectively.**

Figure 6 An example DVH comparison of PTV doses between AAA and Acuros XB(Dm). The dose difference of PTV minimum dose, maximum dose, and mean dose was -3.21%, 4.17% and 0.95%, respectively.
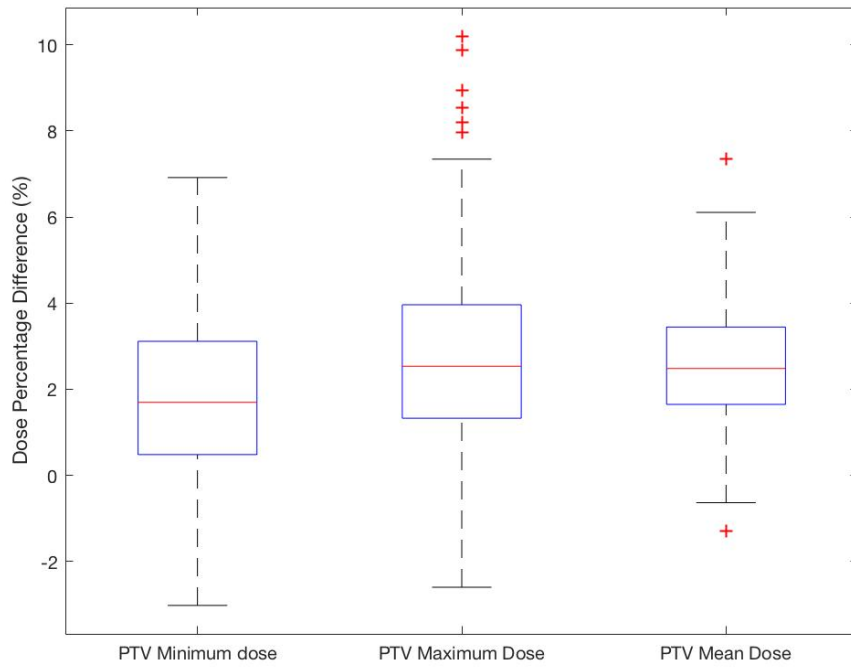
20
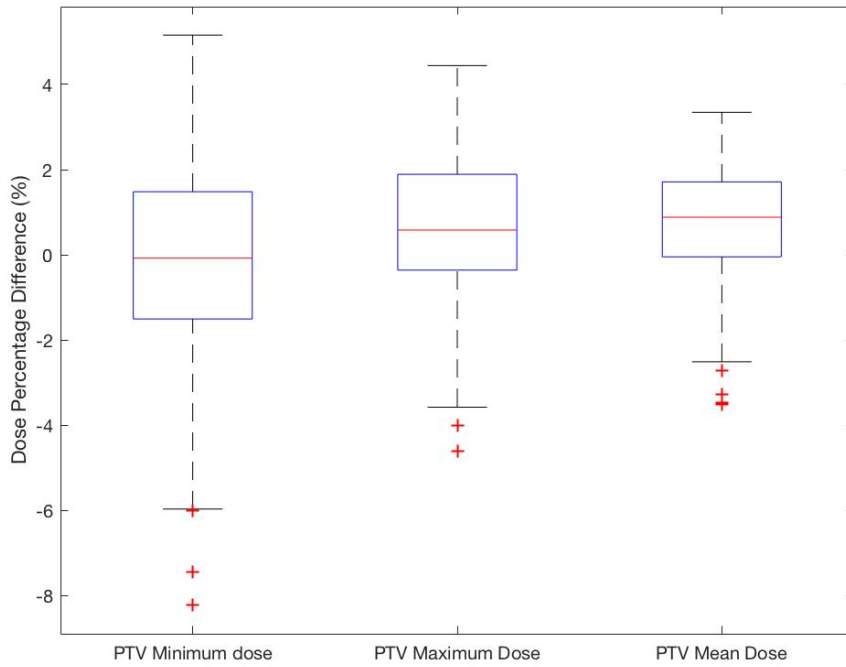
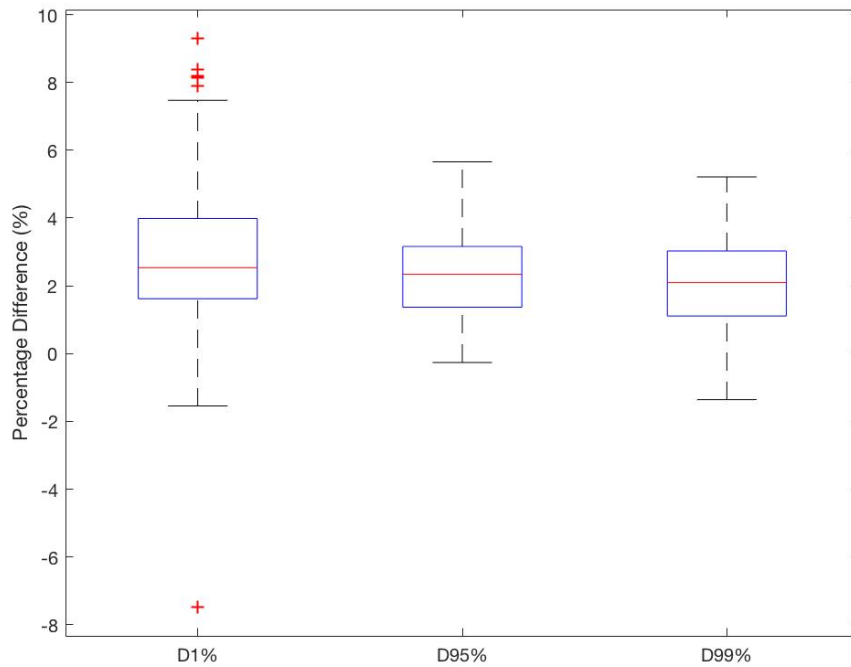**Figure 7 Box plot of PTV dose differences between AAA and Acuros XB(d_m).**
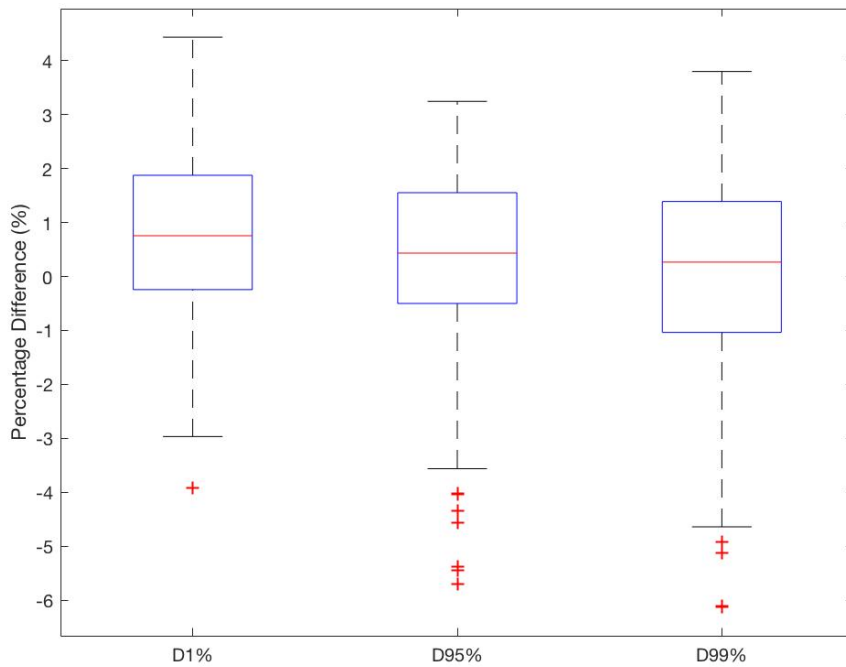
Figure 8 Box plot of difference of dose to 1%, 95%, 99% of PTV between AAA and Acuros XB(d_m).

21

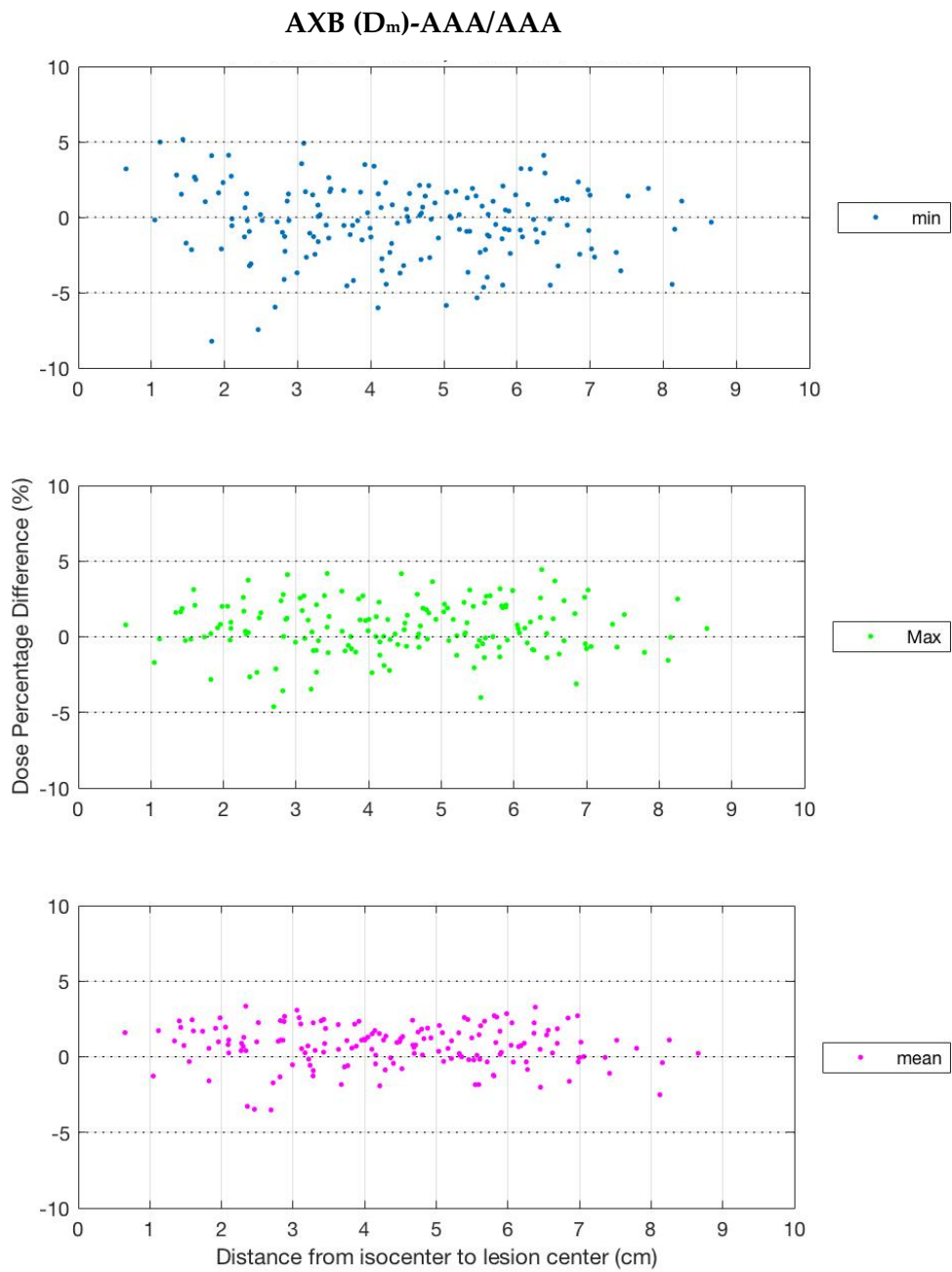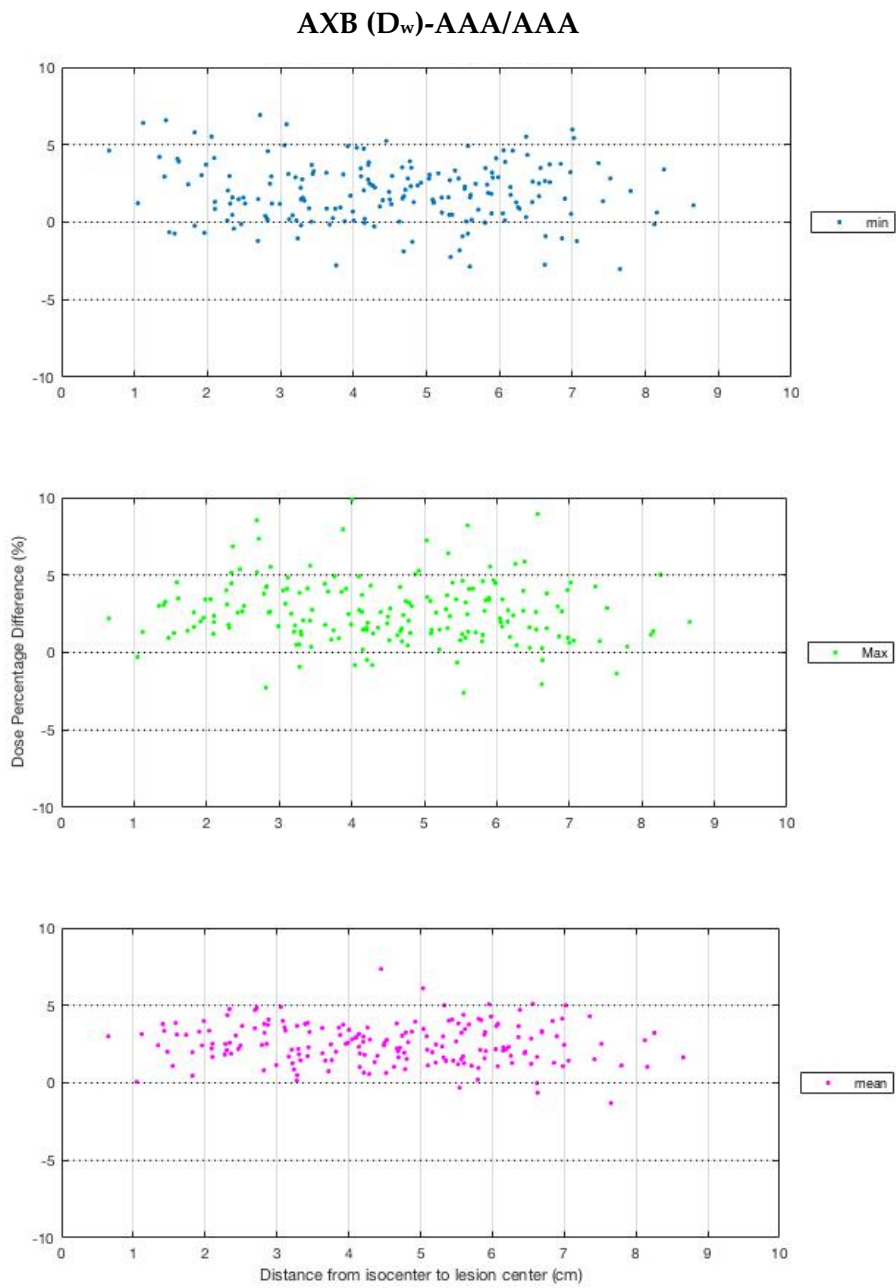**Figure 9 Box plot of PTV dose differences between AAA and Acuros XB(d_w).**

Figure 10 Box plot of difference of dose to 1%, 95%, 99% of PTV between AAA and Acuros XB(d_w).

22

AXB (D$_m$)-AAA/AAA

Figure 11 The scatter plot of dose percentage difference (AXB (D$_m$),AAA) and distance from isocenter to lesion center for PTV dose.

www.manaraa.com

AXB (D$_w$)-AAA/AAA

Figure 12 The scatter plot of dose percentage difference (AXB (D$_w$),AAA) and distance from isocenter to lesion center for PTV dose.

24

AXB (D$_m$)-AAA/AAA

Figure 13 The scatter plot of dose percentage difference (AXB (D$_m$),AAA) and distance from isocenter to lesion center for dose to 1%, 95%, and 99% of the PTV.

AXB (D$_w$)-AAA/AAA

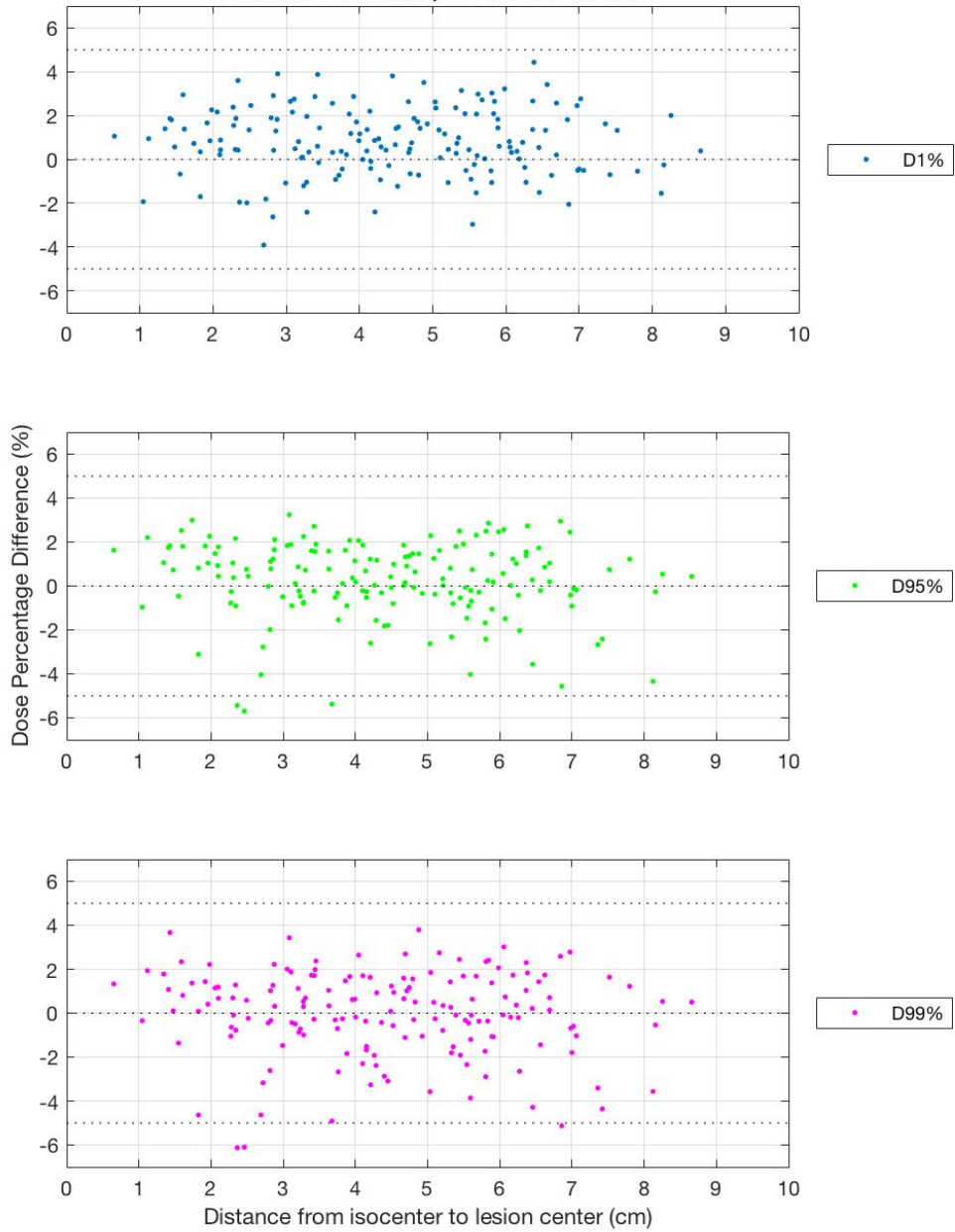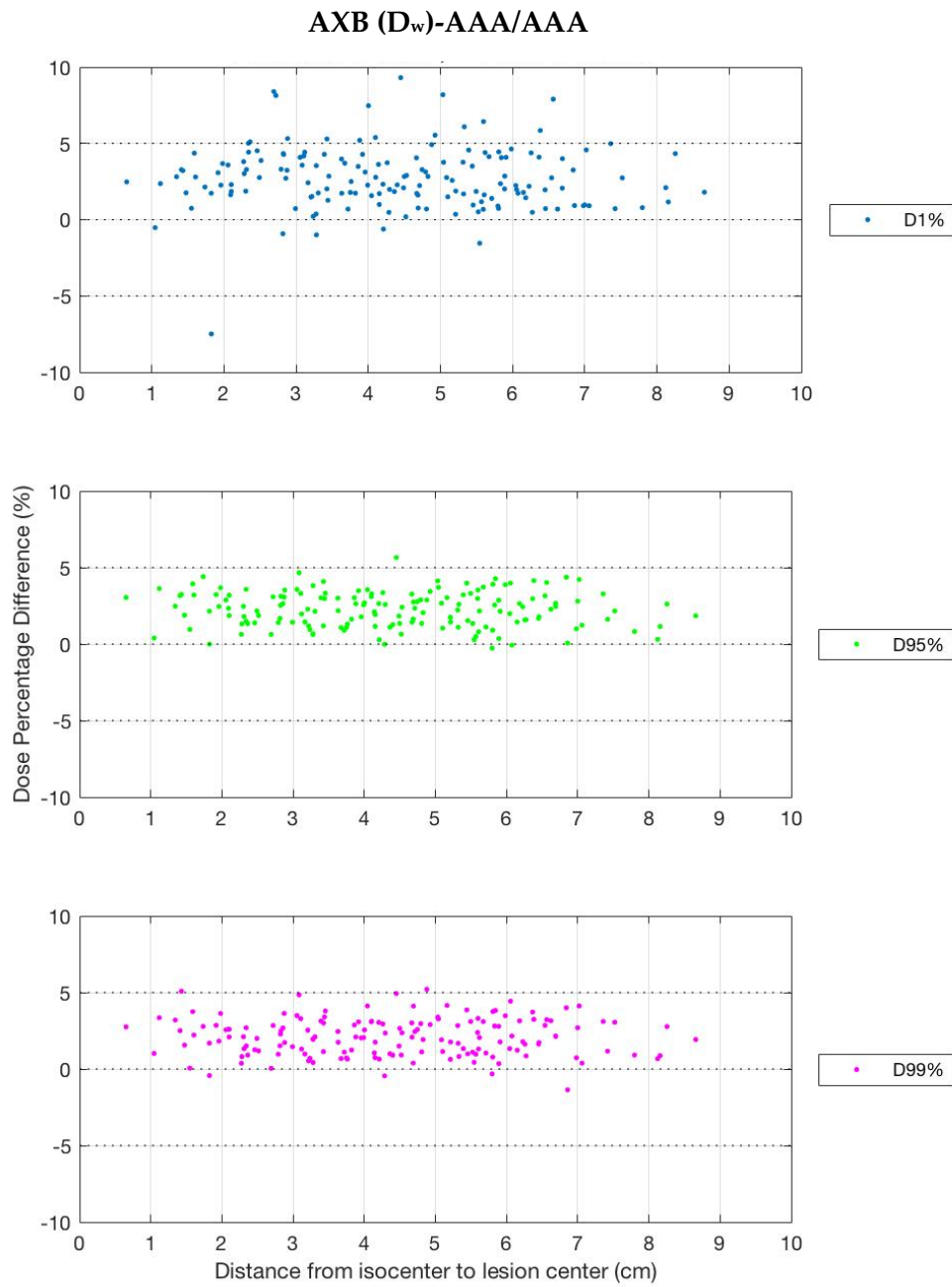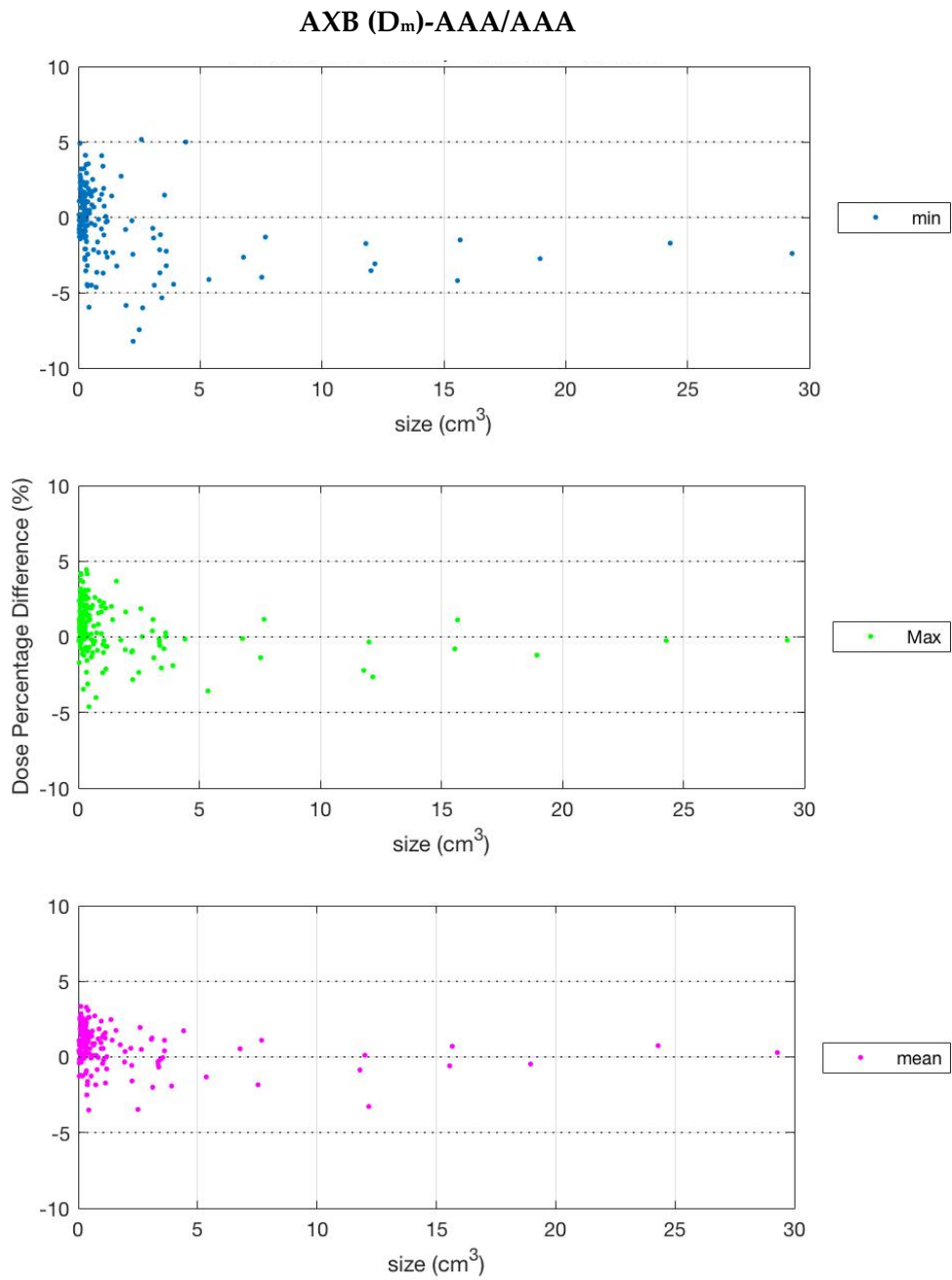**Figure 14 The scatter plot of dose percentage difference (AXB (D$_w$),AAA) and distance from isocenter to lesion center for dose to 1%, 95%, and 99% of the PTV.**

AXB (D$_m$)-AAA/AAA

Figure 15 The scatter plot of dose percentage difference (AXB (D$_m$),AAA) and size for PTV dose.
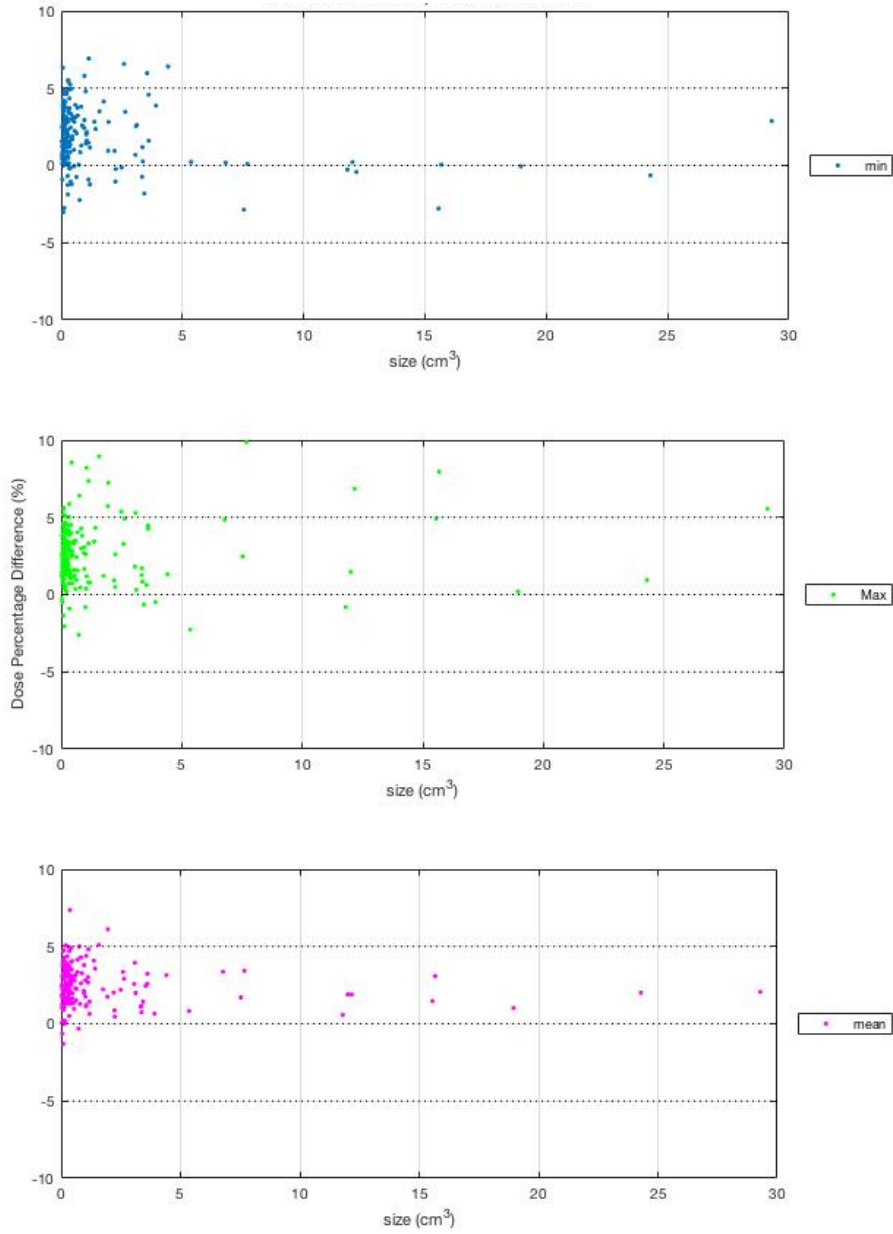
AXB (D_w)-AAA/AAA

Figure 16 The scatter plot of dose percentage difference (AXB (D_w),AAA) and size for PTV dose.
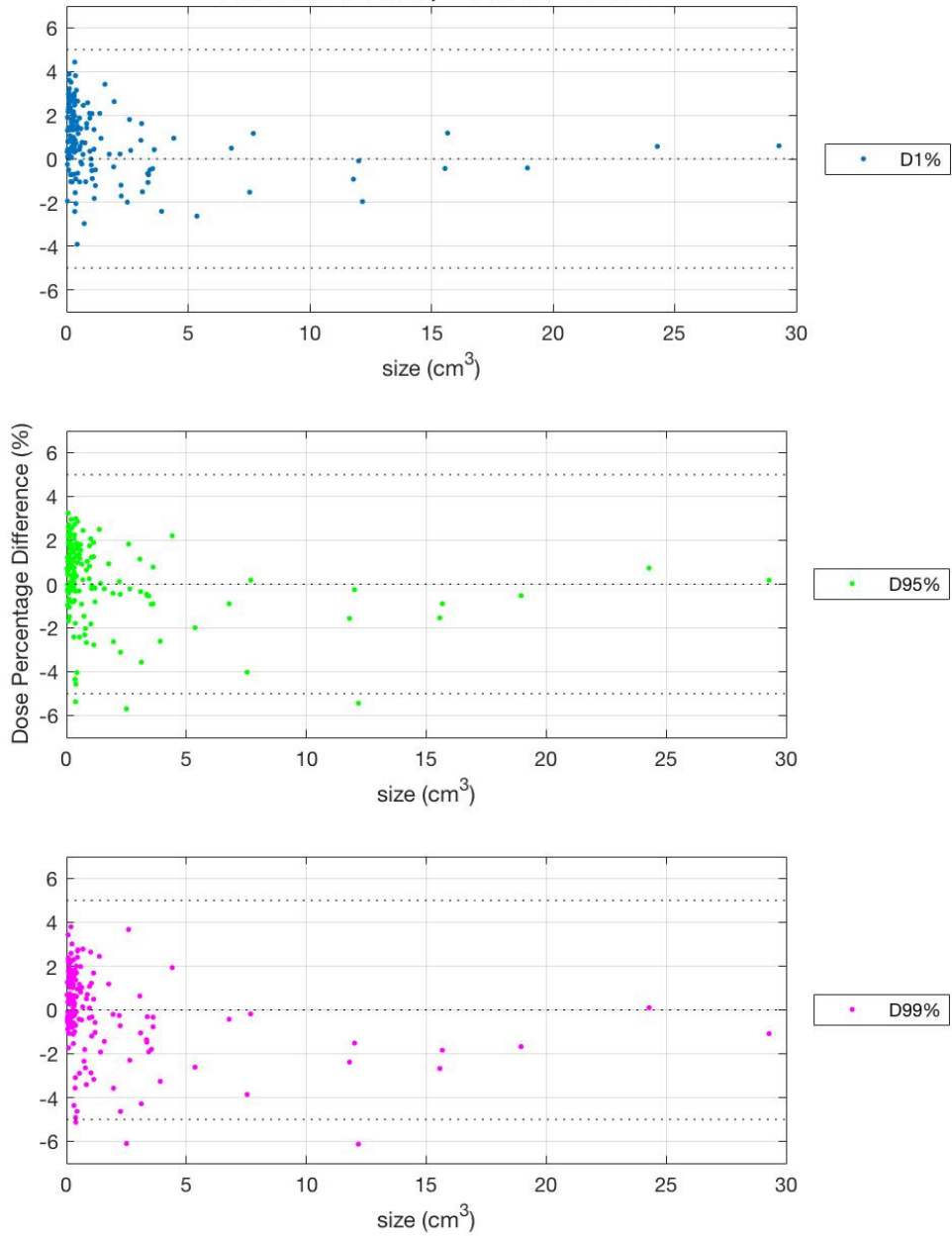
AXB (D$_m$)-AAA/AAA

Figure 17 The scatter plot of dose percentage difference (AXB (D$_m$),AAA) and size for dose to 1%, 95%, and 99% of the PTV.
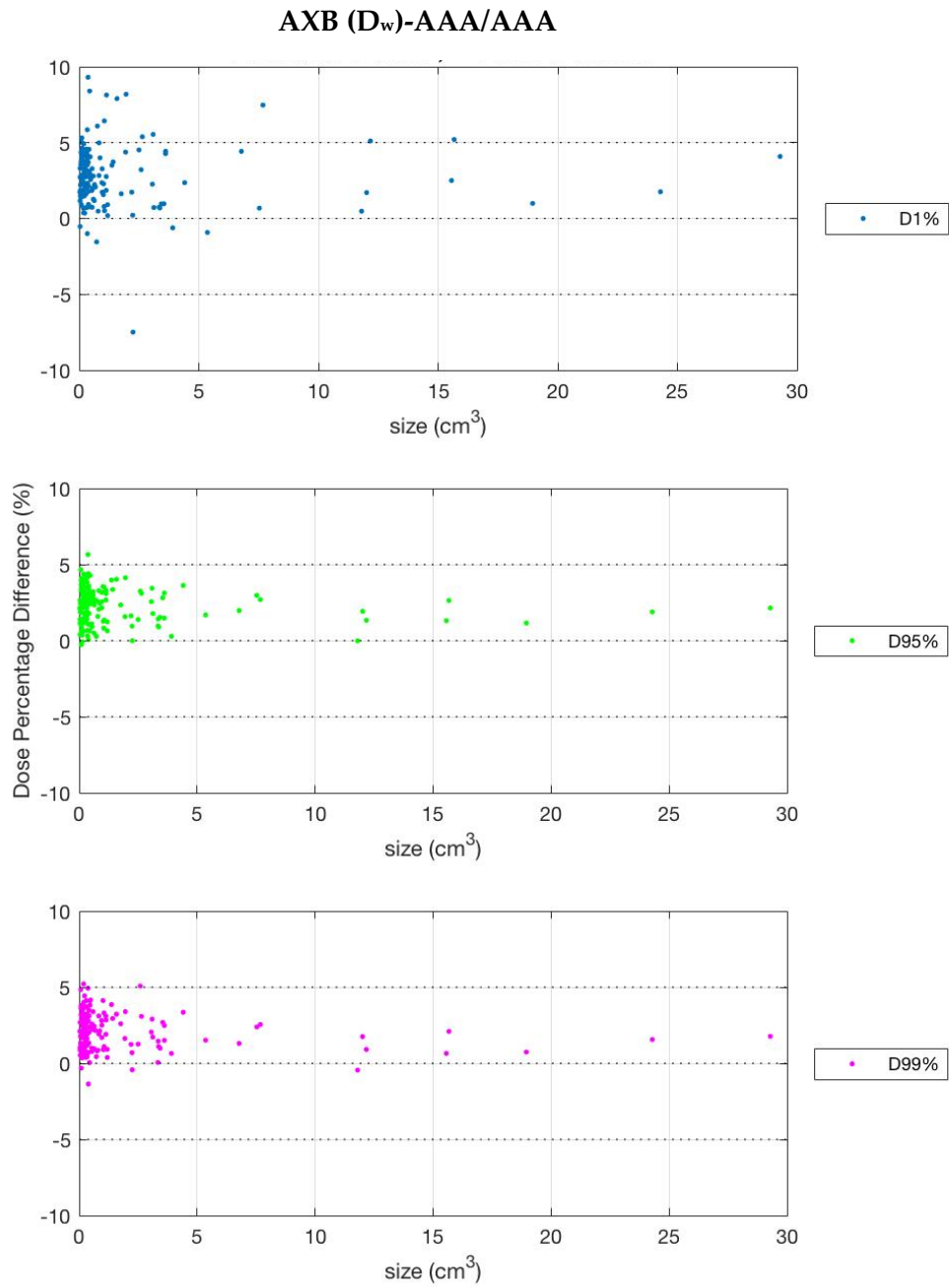
AXB (Dw)-AAA/AAA

Figure 18 The scatter plot of dose percentage difference (AXB (Dw),AAA) and size for dose to 1%, 95%, and 99% of the PTV.
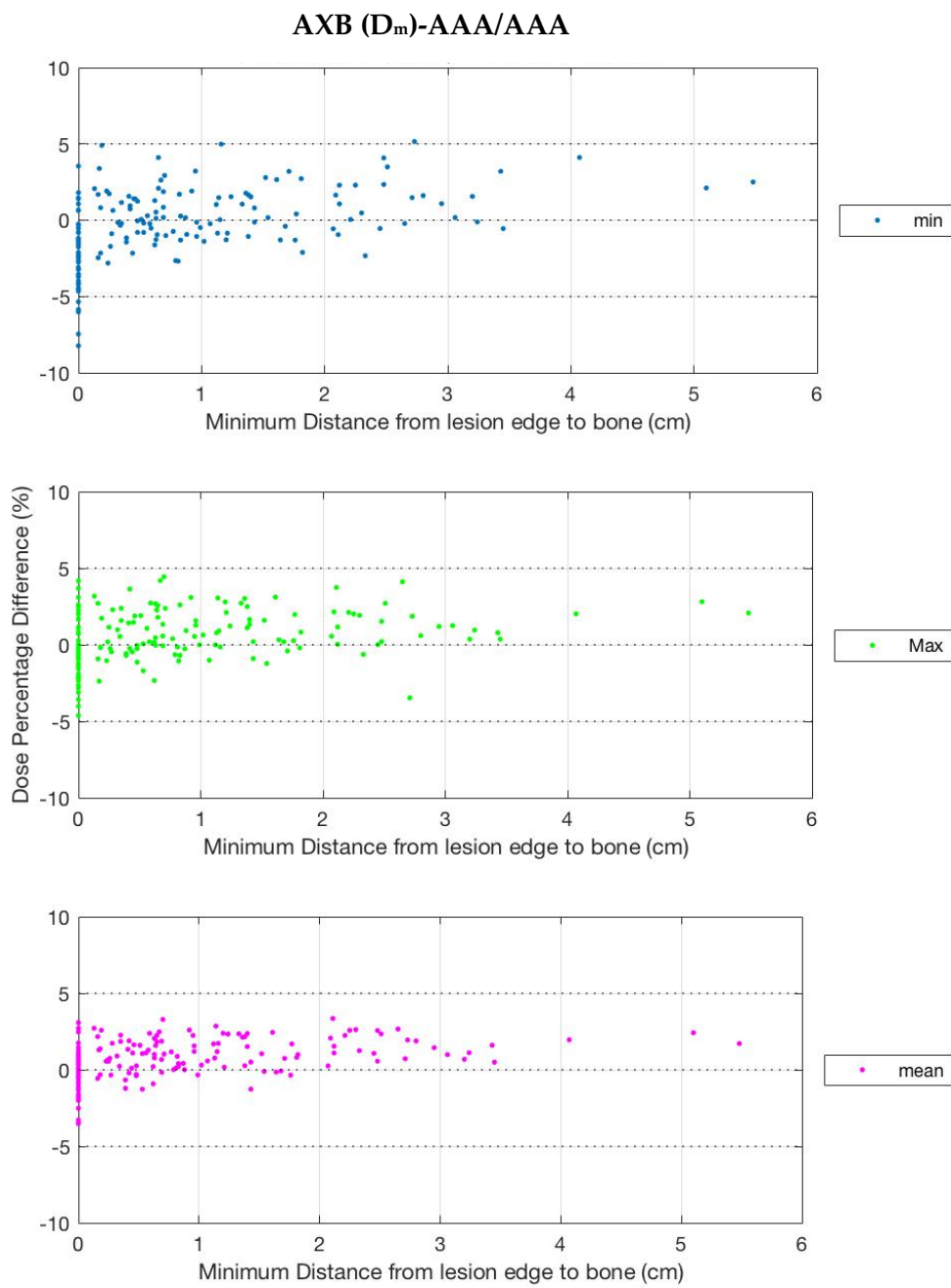
AXB (D$_m$)-AAA/AAA

Figure 19 The scatter plot of dose percentage difference (AXB (D$_m$),AAA) and minimum distance from lesion edge to bone for PTV dose.

AXB (D$_w$)-AAA/AAA

Figure 20 The scatter plot of dose percentage difference (AXB (D$_w$),AAA) and minimum distance from lesion edge to bone for PTV dose.

AXB (D$_m$)-AAA/AAA

Figure 21 The scatter plot of dose percentage difference (AXB (D$_m$),AAA) and minimum distance from lesion edge to bone on dose to 1%, 95%, and 99% of the PTV.
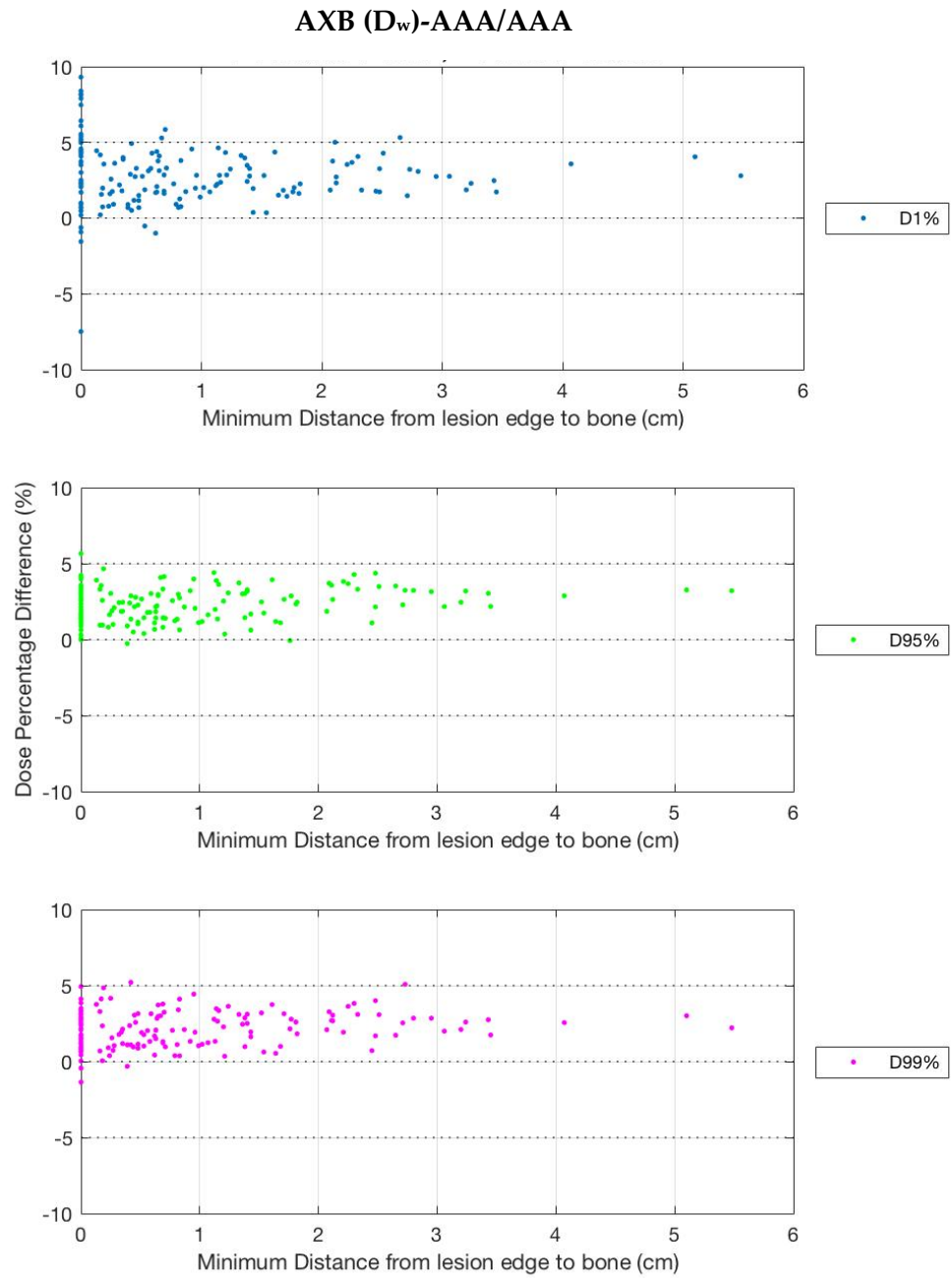
AXB (D$_w$)-AAA/AAA

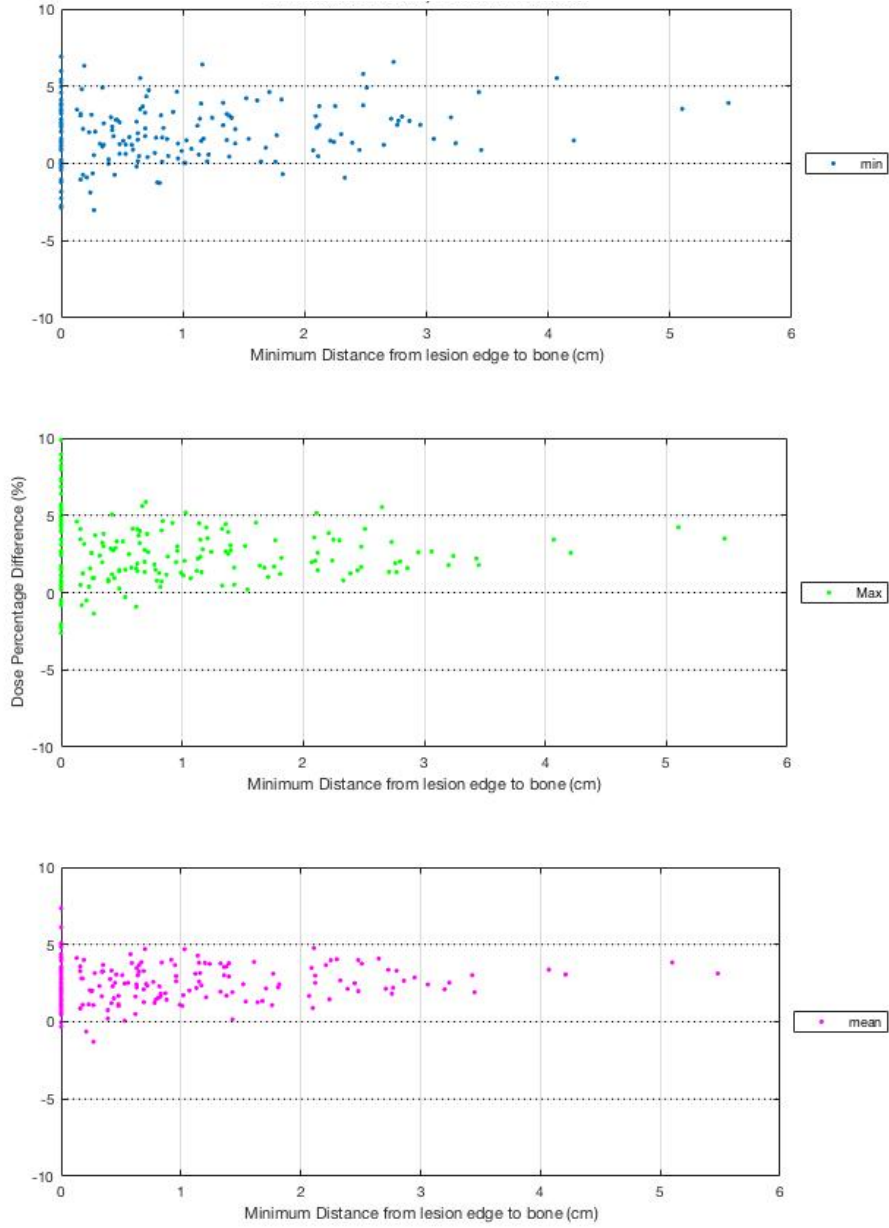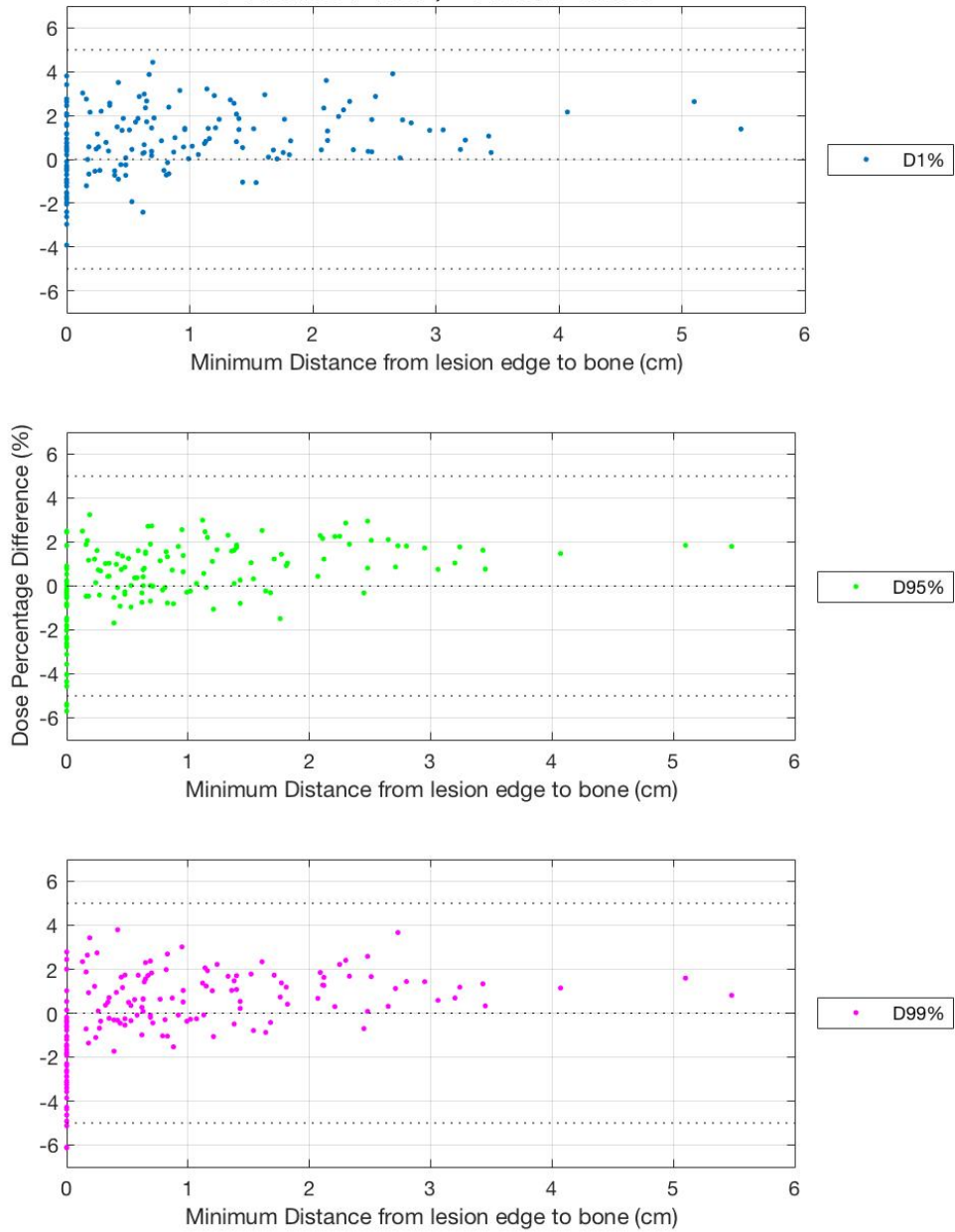Figure 22 The scatter plot of dose percentage difference (AXB (D$_w$),AAA) and minimum distance from lesion edge to bone on dose to 1%, 95%, and 99% of the PTV.

3.1.2 Comparison for brain

Table 4 summarizes the difference for V_{3Gy}, V_{6Gy} and, V_{12Gy}. For D_m and AAA, V_{3Gy} and V_{12Gy} are statistically significant. Figure 21 shows the distribution of the difference of V_{3Gy}, V_{6Gy} and, V_{12Gy}. V_{12Gy} is the most disperse and it is positively skewed. The distribution of V_{6Gy} is symmetric. For V_{3Gy}, most of the differences are negative.

Table 4 Comparison between AAA and Acuros XB for brain

	Relative difference (AXB_D_m-AAA)/AAA*100% Mean ± Std (min-max)	P value	Relative difference (AXB_D_w-AAA)/AAA*100% Mean ± Std (min-max)	P value
Whole brain				
V_{3Gy}	-1.02 ± 0.81 (-3.35 , 0.04)	<0.0001	1.32 ± 0.99 (-0.82 , 3.33)	<0.0001
V_{6Gy}	0.08 ±1.33 (-3.08 , 2.81)	0.11385	3.2 ± 1.62 (-0.16 , 7.85)	<0.0001
V_{12Gy}	2.77 ± 2.74 (-2.27, 10.34)	<0.0001	6.00 ± 3.55 (-5.81 , 14.64)	0.0004

35
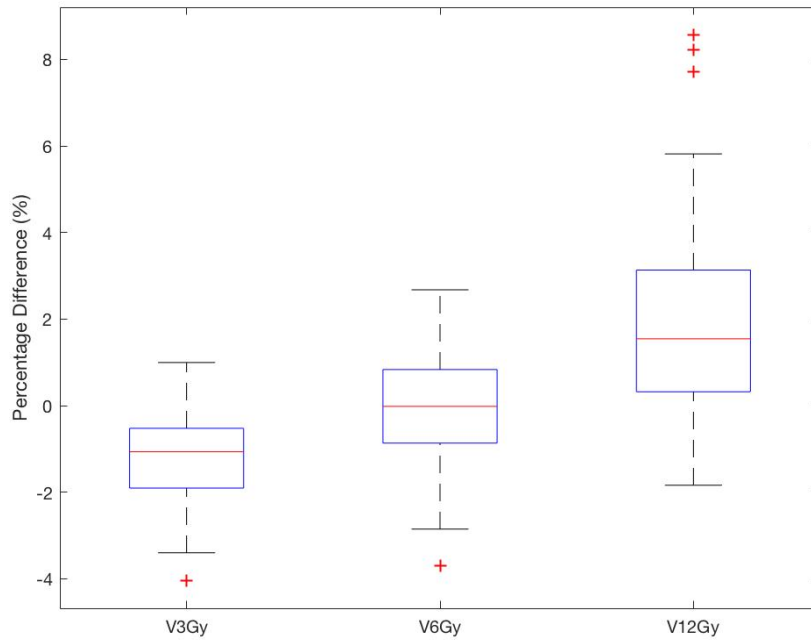
Figure 23 Box plot of the difference of V_{3Gy}, V_{6Gy} and V_{12Gy} between AAA and Acuros XB(d_m)
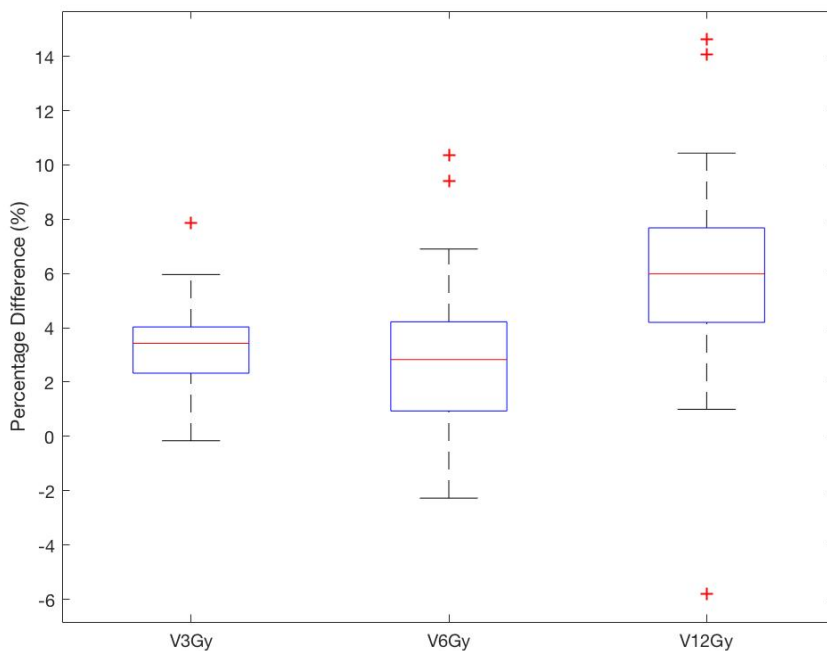
Figure 24 Box plot of the difference of V3Gy, V6Gy and V12Gy between AAA and Acuros XB(d_w)

36

3.2 Dosimetric Accuracy

Figure 13 shows the calculated dose from the AAA and Acuros XB and measured dose by using SRS MapCHECK. The average of the percentage difference between AAA and measurement is -1.14%, while the average of the percentage difference between Acuros XB and measurement is -5.79% (Table 6). The results showed that the AAA is close to the measurements and better compared to the Acuros XB.
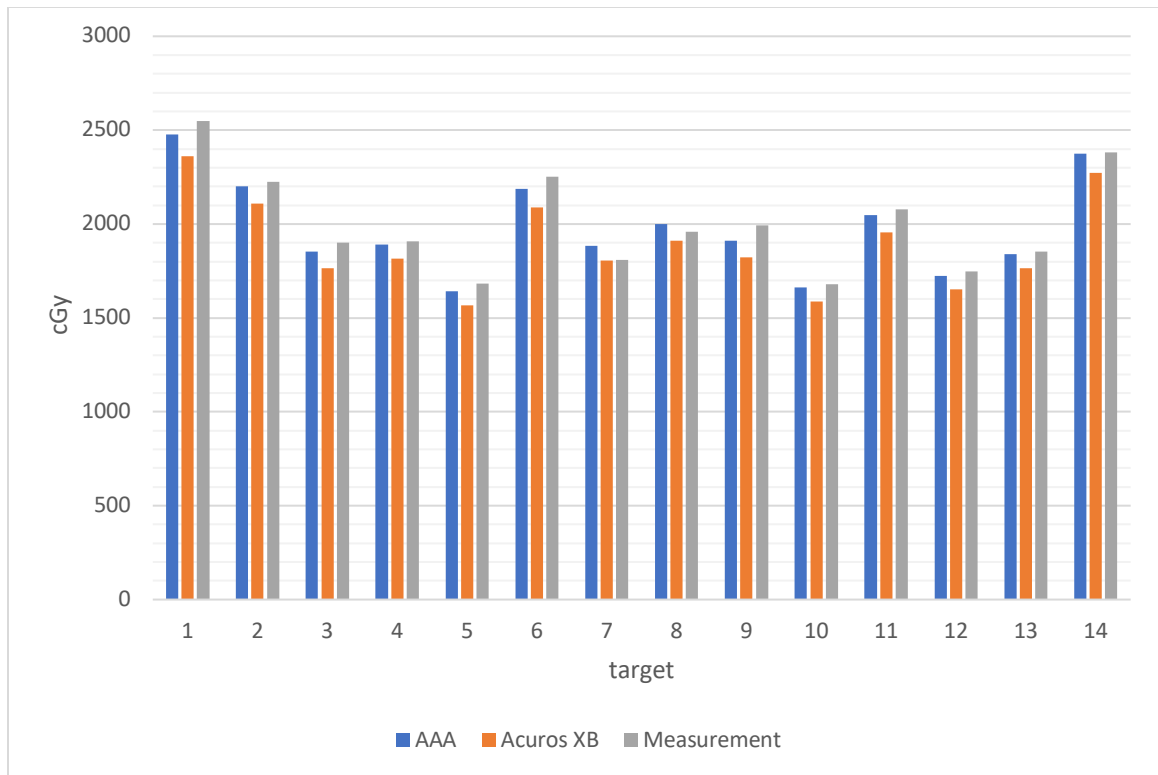
Figure 25 Calculated dose from AAA and Acuros XB and measurement.

Table 5 Dose percentage differences between measurement and AAA or Acuros XB

| | Percentage Difference (%) | | |
	Mean	Std	Range
AAA	-1.14	2.00	-4.17 , 3.93
AXB	-5.79	2.24	-9.33 , -0.33

Table 6 Gamma passing rates comparing measurement and calculated dose

| | Gamma Pass Rate(%) | | |
	Mean	Std	Range
AAA	99.9	0.17	99.4 , 100
AXB	97.9	2.11	93.6 , 100

38

4. Discussion

Since Acuros XB has been introduced for years, relatively few studies have investigated its performance in SRS treatments. Most of them focused on SBRT lung cases. The purpose of this project is to compare the dose calculated by two algorithms AAA and Acuros XB with clinical brain metastases cases, which represent heterogeneities and usually use small fields. The AAA and Acuros XB plans were evaluated based on the results derived from the Dose Volume Histogram (DVH) in the Eclipse TPS. Moreover, the dosimetry accuracy was assessed by performing SRS MapCHECK measurement and comparing the measurement and the planned doses.

The considerable dose discrepancies were found in PTV minimum dose and $D_{99\%}$. These discrepancies demonstrated that the delivered dose is insufficient when the patient's plan would have been calculated by AAA. These differences can be explained by the poor prediction in the secondary build-up region where to re-establish electronic equilibrium beyond low-density media (Rana 2013, Bush 2011, Fogliata 2011). However, the Acuros XB has better dose prediction under the electronic disequilibrium conditions.

The large dose discrepancies were also found when the distance from lesion edge to bone was small or when tumor size was small. The small tumor size may be treated by small fields. The small field usually introduces uncertainty due to the absence of particle equilibrium conditions. Moreover, the short distance might affect how dose calculation algorithms manage heterogeneity and result in large dose discrepancies.

39

Both Acuros XB(d_m) and Acuros XB(d_w) showed a slight but significant ($p < 0.05$) higher V_{12Gy} (volume of the brain receive 12Gy or more) value than AAA. The differences in brain doses calculated by AAA and Acuros XB were dependent on patient since field size and PTV location inside the brain affect dose calculations. Therefore, clinical uncertainty for the value of V_{12Gy} exist depending on the choice of dose calculation algorithm.

Regarding dosimetric accuracy, AAA agreed better than Acuros XB with SRS MapCHECK measurements. The dose calculation was performed based on the CT images of phantom and detectors. That the phantom is made of homogenous media may not be able to compare two dose calculation algorithms in terms of management of heterogeneity. In addition, the high density materials in the SRS MapCHECK detectors are metal, which does not represent the clinical case for patients, and the Acuros algorithm may recognize the high density as different material. and result in incorrect calculation.

Both Monte Carlo dose calculation and Acuros XB report d_m and d_w. Some studies suggest that dose-to-medium should be reported when Monte Carlo dose calculation or other Boltzmann solver (e.g., Acuros XB) are used. (2002 Liu, 2011 Ma, 2016 Gladstone) From our comparison, although the differences between AAA and d_m were smaller than the mean differences between AAA and d_w, the differences revealed up to 6%. These differences can be serious since physicians prescribe dose to isodose

40

line. If the prescription dose is the same, it could potentially make the MU differ by a

few percentage depending on the choice of reporting mode or on the choice of dose

calculation algorithms.

41

5. Conclusion

The results of clinical data showed a significant difference for mean dose, maximum dose, $D_{1\%}$, CI and HI of PTV. Sizable dose differences were found in AAA and Acuros XB(d_m), particularly in the PTV minimum dose and PTV coverage. Differences between AAA and Acuros XB(D_m) were generally less than differences between AAA and Acuros XB(D_w). Heterogeneity and tumor size introduced uncertainty for dose calculation. However, the dose difference showed no dependence on the distance from isocenter to lesions. The results of the measurement study showed a better agreement with the calculation of AAA than Acuros XB.

References

Patchell RA. The management of brain metastases. *Cancer Treatment Reviews.* 2003;29(6):533-540.

Brown PD, Jaeckle K, Ballman KV, et al. Effect of Radiosurgery Alone vs Radiosurgery With Whole Brain Radiation Therapy on Cognitive Function in Patients With 1 to 3 Brain Metastases. *Jama*. 2016;316(4):401.

Tsao M, Xu W, Sahgal A. A meta-analysis evaluating stereotactic radiosurgery, whole-brain radiotherapy, or both for patients presenting with a limited number of brain metastases. *Cancer*. 2011;118(9):2486-2493.

Yamamoto M, Serizawa T, Shuto T, et al. Stereotactic radiosurgery for patients with multiple brain metastases (JLGK0901): A multi- institutional prospective observational study. *Lancet Oncol*. 2014; 15:387-395.

Jairam V, Chiang V, Yu J, Knisely J. Role of stereotactic radiosurgery in patients with more than four brain metastases. *CNS Oncol*. 2013; 2(2):181–193.

Clark GM, Popple RA, Young PE, Fiveash JB. Feasibility of single- isocenter volumetric modulated arc radiosurgery for treatment of multiple brain metastases. *Int J Radiat Oncol Biol Phys*. 2010;76:296- 302.

Kim H, Choi J, Lee S, Sung K, Lee S, Lee K. Volumetric modulated arc therapy for multiple brain metastases: A more efficient modality than dynamic arc stereotactic radiosurgery. *Int J Radiat Oncol Biol Phys*. 2012;84:S787.

Tillikainen L, Siljamaki S, Helminen H, Alakuijala J, Pyyry J. Determination of parameters for a multiple source model of megavoltage photon beams using optimization methods. *Phys Med Biol*. 2007;48:1441–1467.

Fogliata A, Nicolini G, Clivio A, Vanetti E, Mancosu P, Cozzi L. Dosimetric validation of the Acuros XB advanced Dose Calculation algorithm: fundamental characterization in water. *Phys Med Biol*. 2011;56:1879–1904.

Fogliata A, Nicolini G, Vanetti E, Clivio A, Cozzi L. Dosimetric validation of the anisotropic and analytical algorithm for photon dose calculation: fundamental characterization in water. *Phys Med Biol*. 2006;51:1421–1438.

Wareing TA, McGhee JM, Morel JE, Pautz SD. Discontinuous finite element Sn methods on three-dimensional unstructured grids. *Nucl Sci Eng*. 2001;138:256–268.

43

Bush K, Gagne IM, Zavgorodni S, Ansbacher W, Beckham W. Dosimetric validation of Acuros XB with Monte Carlo methods for photon dose calculations. *Med Phys*. 2011;38:2208–21.

Fogliata A, Nicolini G, Clivio A, Vanetti E, Cozzi L. Dosimetric evaluation of Acuros XB Advanced Dose Calculation algorithm in heterogeneous media. *Radiat Oncol*. 2011;6:82.

Rana, Suresh, and Kevin Rogers. "Dosimetric evaluation of Acuros XB dose calculation algorithm with measurements in predicting doses beyond different air gap thickness for smaller and larger field sizes." *Journal of medical physics* vol. 38,1 (2013): 9-14.

Shaw E, Kline R, Gillin M, et al. Radiation Therapy Oncology Group: radiosurgery quality assurance guidelines. *Int J Radiat Oncol Biol Phys*. 1993;27(5):1231–39.

Eichler AF, Loef er JS. Multidisciplinary management of brain metastases. *The Oncologist*. 2007;12(7):884–98.

Feuvert L, Noël G, Mazeron JJ, Bey P. Conformity index: a review. *Int J Radiat Oncol Biol Phys*. 2006;64(2):333–42.

Low DA, Harms WB, Mutic S, Purdy JA. A technique for the quantitative evaluation of dose distributions. *Medical Physics*. 1998;25(5):656-661.

Liu HH. Dm rather than Dw should be used in Monte Carlo treatment planning. For the proposition. *Med Phys*. 2002;29: 922–923.

Ma C, Li J. Dose specification for radiation therapy: dose to water or dose to medium. *Phys Med Biol*. 2011;56:3073–3089.

Gladstone DJ, Kry SF, Xiao Y, Chetty IJ. Dose specification for NRG radiation therapy trials. *Int J Radiat Oncol Biol Phys*. 2016;95:1344– 1345

44